

Investigation of ZnO nanotubes array as an antireflective coating for planar CZTS/ZTO solar cell

adnen melliti (✉ adnenmelliti@yahoo.fr)

Universite de Tunis Ecole Nationale Superieure d'Ingenieurs de Tunis <https://orcid.org/0000-0003-4233-6939>

Research Article

Keywords: CZTS, ZnO, ZTO, RCWA, solar cell, nanotube, antireflective coating

Posted Date: May 6th, 2021

DOI: <https://doi.org/10.21203/rs.3.rs-462226/v1>

License:  This work is licensed under a Creative Commons Attribution 4.0 International License.

[Read Full License](#)

Investigation of ZnO nanotubes array as an antireflective coating for planar CZTS/ZTO solar cell

Adnen Melliti^{1,2}

¹Université de Carthage, Institut Préparatoire aux Etudes Scientifiques et Techniques, Laboratoire Matériaux-Molécules et Applications, BP51 La Marsa 2070, Tunisia.

²Université de Tunis, Ecole Nationale Supérieure des Ingénieurs de Tunis, 5 Rue Taha Hussein – Montfleury – 1008 Tunis, Tunisia.

Abstract

We present a theoretical investigation of ZnO nanotubes square periodic array as an antireflective coating for a planar solar cell including Kesterite as a p-type absorber and Zinc Tin Oxide as an n-type buffer. The method of the calculation is rigorous coupled wave analysis. We found that this coating leads to a considerable reduction of the loss of the ideal short circuit current density by about 80 %. The optimal values of the nanotube diameter, nanotube height, array period and the absorber thickness are 438 nm, 150 nm, 438 nm and 1.5 μm respectively. The study of the variation of the loss of the ideal short circuit current density with the incident angle of the sunlight shows that the NTs array still has good anti-reflection characteristics as long as the incident angle doesn't exceed 60°.

Keywords: CZTS; ZnO; ZTO; RCWA; solar cell; nanotube; antireflective coating

1- Introduction

Recently, nanostructures, such as nanowires and nanotubes (NTs), have attracted considerable attention due to their importance in potential technological applications such as field emission devices [1], photocatalysis [2], sensors [3-5] and solar cells (SCs) [6-9]. Indeed, nanostructures

can increase the absorption of the light, due to the trapping effect, by optimization of the geometrical parameters [8-10]. Furthermore, experimental research on InGaP/GaAs/Ge solar cell used ZnO nanotubes as antireflective coating (ARC) to improve the efficiency of the solar cells [11]. Indeed, the coating with a NT- film minimizes the reflected light at the front surface and thus increases the absorbed energy due to the gradual variation of the refractive index.

In this paper, we study the effect of ZnO NTs array as an antireflective film on the surface of thin films SC including Kesterite $\text{Cu}_2\text{ZnSnS}_4$ (CZTS) as a p-type absorber and Zinc Tin Oxide (ZTO) as an n-type buffer. Indeed, CZTS has outstanding electrical and optical features as a direct optical band gap of 1.5 eV [9] and ZTO has high transmittance in the visible range [8]. Furthermore, the p-CZTS-n-ZTO heterojunction has a favorable conduction band alignment and is only consisting of earth-abundant and non-toxic constituents. The use of NT array antireflective help To improve the CZTS thin film SC performance, especially the power conversion efficiency of this SC (9.3 % [12] is relatively weak compared to the one reported for CIGS thin film SC (22.9 %) [13].

The optical simulation was made using rigorous coupled wave analysis (RCWA) with Pavel Kwiecien's rcwa-2d code for MATLAB (sourceforge.net/projects/rcwa-2d/), based on [14]. The validation of the used code was made in previous work [8]. To minimize its value, we calculated the loss of the ideal short circuit current density, due to the reflection on the ZnO NTs array, as a function of the NTs diameter and the ratio between the period array and the NTs diameter for different values of NTs height. The maximal value obtained for the ideal short circuit current density (J_{ph}) is about 41 % greater than that of a planar SC without NTs array. A study of the variation of ideal current density with the incident angle of the light is also reported.

According to our best knowledge, an optical simulation of solar cell based on CZTS thin film with ZnO NTs array as antireflective has been reported for the first time in the present study.

In section 2, we described the structure of the SC simulated. Section 3 is devoted to the optimization of the geometrical parameters of NTs array to minimize the loss of the ideal short circuit current due to the reflection on the surface. The fourth section is reserved to study the variation of this current with the incident angle of the light.

2. Device setup

The structure of the SC covered by a ZnO square periodic array of NTs investigated in this article is shown in figure 1. The period, diameter and height of the NTs array are denoted by P,

D and h respectively. The thickness of the wall of the NTs is 20 nm according to experimental measures [10]. The NTs are deposited on n-ZnO seed layer of 0.5 μm thickness which covers a $\text{Zn}_{0.77}\text{Sn}_{0.23}\text{O}$ (buffer layer)-CZTS (absorber) heterojunction. The composition of Sn and the thickness of the buffer layer (10 nm) were chosen to obtain a good CZTS solar performance [8]. The thickness of the absorber layer was varied during the optical simulation. The p-CZTS layer is electrically connected to the device contact by a 0.3 μm FTO layer.

The values of the refractive index and extinction coefficient of ZTO, CZTS, ZnO and FTO were taken from references [15-18].

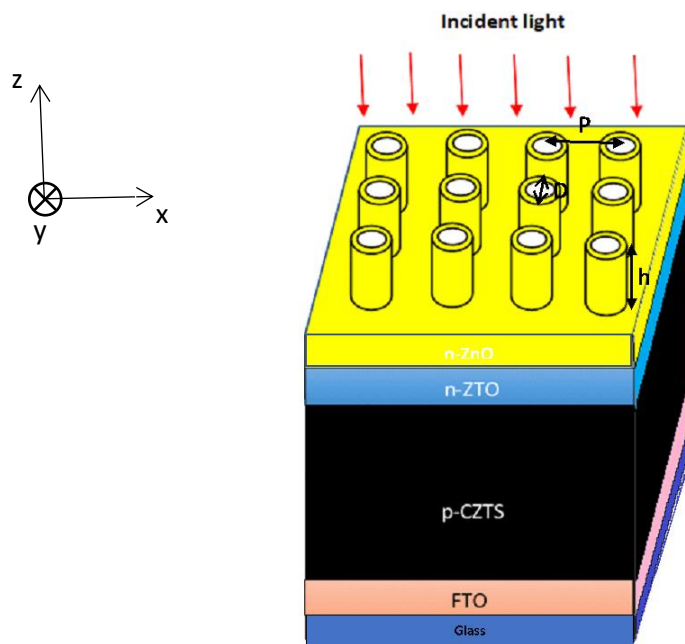


Figure 1: Structure of the planar SC including CZTS as p-type absorber and ZTO as n-type buffer with a ZnO NTs array as an anti-reflector.

2 Optimization of the geometrical parameters of the NTs array

To highlight the effect of the NTs array on the reflectance by the SC surface, we presented on figure 2 the reflectance spectra obtained for SCs coated or not coated by NTs array. We note a significant decrease of the reflectance by the coating by a NTs array. Furthermore, we remark that the resonances of both spectra are located at the same wavelengths in the range of 0.55 to 0.9 μm . On the other hand, in the range of 0.3 to 0.55 μm the positions of the resonances of both spectra are different.

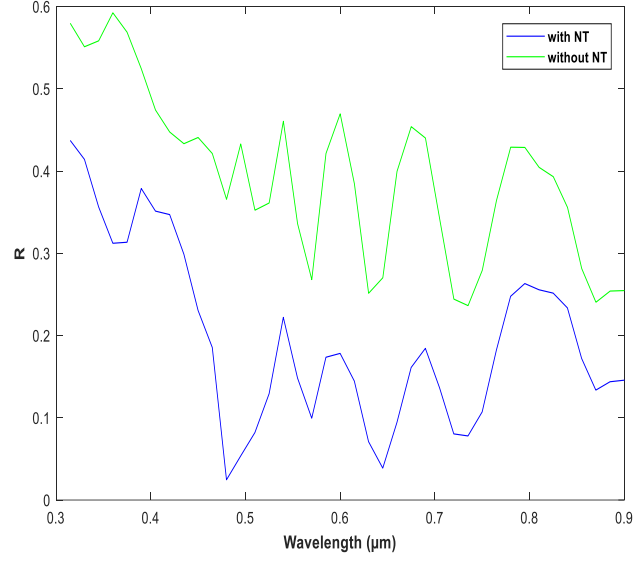


Figure 2: Reflectance spectra of SCs with and without NTs array. The height, the diameter of NTs, the period of the array and the thickness of the CZTS layer are 150 nm, 240 nm, 480 nm and 1 μm .

To optimize the geometrical parameters of the NTs array, we calculated the lost ideal short circuit current density due to the reflection on the NTs array (J_{phR}). We express this loss by the following integral:

$$J_{phR} = \frac{e}{h \cdot c} \int_{300}^{\lambda_g} R(\lambda) \cdot I(\lambda) \cdot \lambda \cdot d\lambda$$

where $R(\lambda)$ is the wavelength-dependent reflectance, $I(\lambda)$ denotes the ASTM AM1.5G solar irradiance taken from Ref. [19], e , h , and c are fundamental physics constants: electron charge, Plank constant, and light celerity, respectively. The integration has been performed every 0.01 μm from 300 nm to the wavelength of the threshold of absorption of the absorber layer ($\lambda_g = 0.826 \mu\text{m}$). We chose to begin the integration from 300 nm because the solar power is very weak below this wavelength.

To determine the optimal values of the geometrical parameters of the NTs array, we calculated J_{phR} as a function of the NTs diameter (D) and the ratio between the period array and the NTs diameter (P/D) for different values of NTs height (h). In figure 3.a, we presented the mapping obtained for $h = 150 \text{ nm}$. The results obtained from all calculated mappings are summarized in figure 3.b. We remark that with increasing h , the optimal value of the NTs diameter first increases rapidly. Then, it oscillates. On the other hand, J_{phR} decreases rapidly, due to the increase of the effect of NTs array, and reaches a minimum value, 3.5 mA/cm^2 , for $h = 150 \text{ nm}$.

Then, it oscillates and remains constant for h greater than 600 nm. Furthermore, for all values of h , the optimal value of P/D is 1.

The minimum value of $J_{ph}R$, 3.5 mA/cm^2 , is obtained for $h=150 \text{ nm}$, $D = 438 \text{ nm}$ and period = 438 nm . The value of $J_{ph}R$ obtained for SC without NTs array coating is 17 mA/cm^2 . Then the percentage of the reduction of $J_{ph}R$ due to the deposition of NTs array on the surface of the solar cell is 80%.

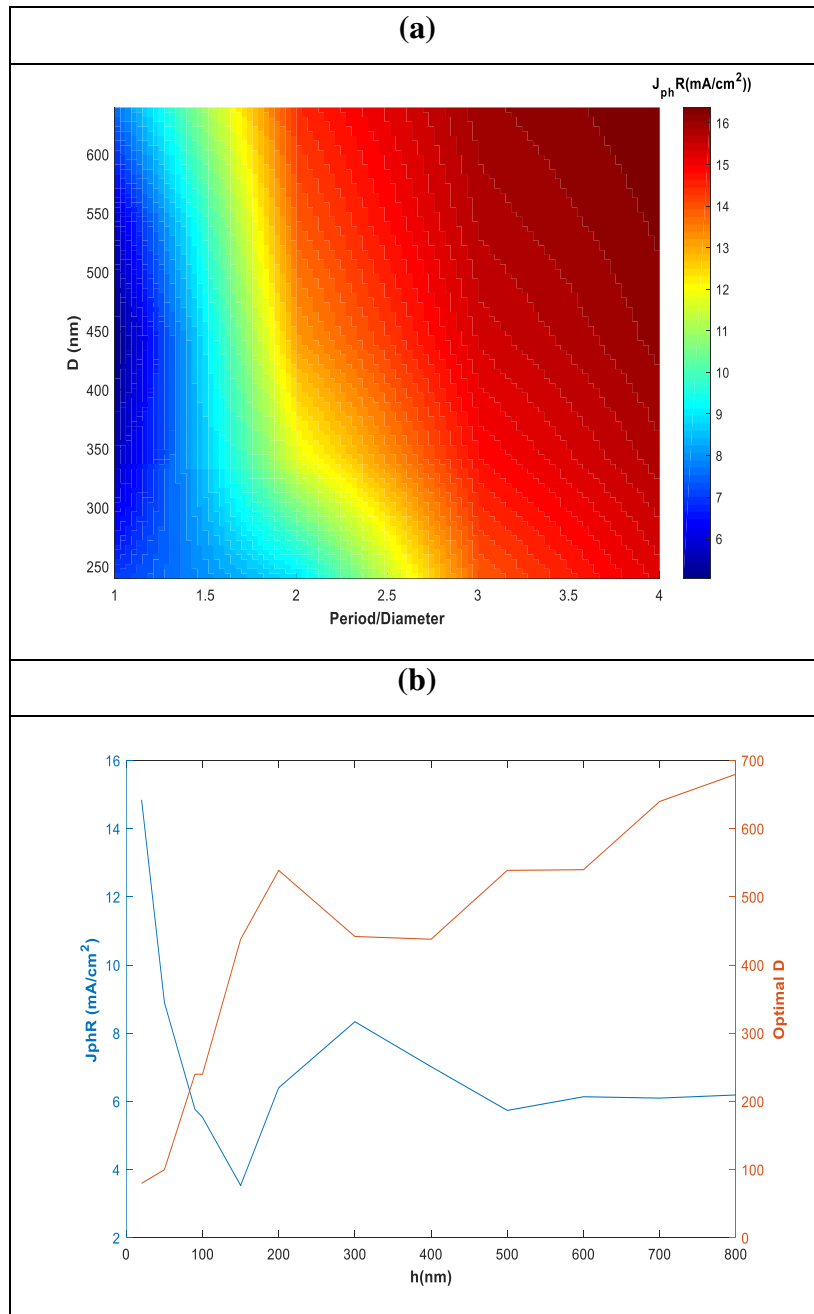


Figure 3: (a) Lost ideal short circuit current density ($J_{ph}R$) computed for $h = 150$ nm as a function of the diameter of NTs (D) and the ratio between the array period P and the diameter D of the NTs. The 20 data points map has been linear interpolated on a 500 times larger grid. The thickness of the CZTS layer is $1 \mu\text{m}$. **(b)** Evolution of the optimal value of the NTs diameter and the corresponding value of $J_{ph}R$ as a function of NTs height (h).

To optimize the value of the thickness of the absorber layer (t_{CZTS}), we presented on figure 4 the evolution of the value of the ideal short circuit current density (J_{ph}) of the investigated SC with and without NTs array as a function of t_{CZTS} . The values of the geometrical parameters of NTs array are the optimal values. We note that J_{ph} increases with the thickness of the absorber layer and remains constant from $1.5 \mu\text{m}$. Then, this value can be considered as the optimal value. On the other hand, we remark that the use of NTs array to cover the surface of the SC permits to increase J_{ph} from 29 to 41 mA/cm^2 , in other words, by about 41 %.

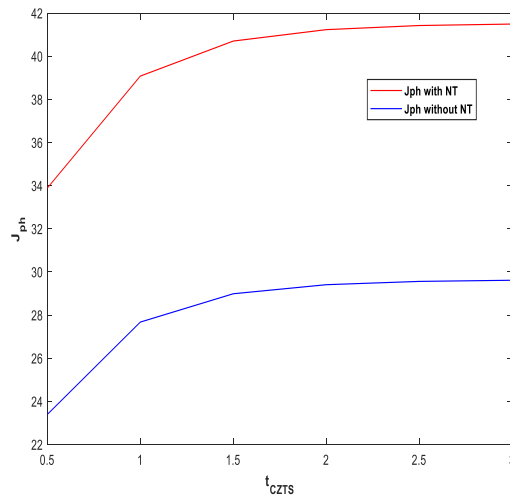


Figure 4: Variation of ideal short circuit current density (J_{ph}) obtained for the optimal values of D and P/D as a function of the thickness of the CZTS layer (t_{CZTS}).

On figure 5, we presented the Component E_x of the electric field at a wavelength of $0.5 \mu\text{m}$ in the SCs with and without NTs array. The values of the geometrical parameters of the NTs array are the optimal values. We remark that in the absence of NTs array, we obtain a good interference figure on the surface of the SC. With the coating with a NTs array, the interference figure is perturbed and the light intensity, the resultant of the incident and reflected light, decreases considerably.

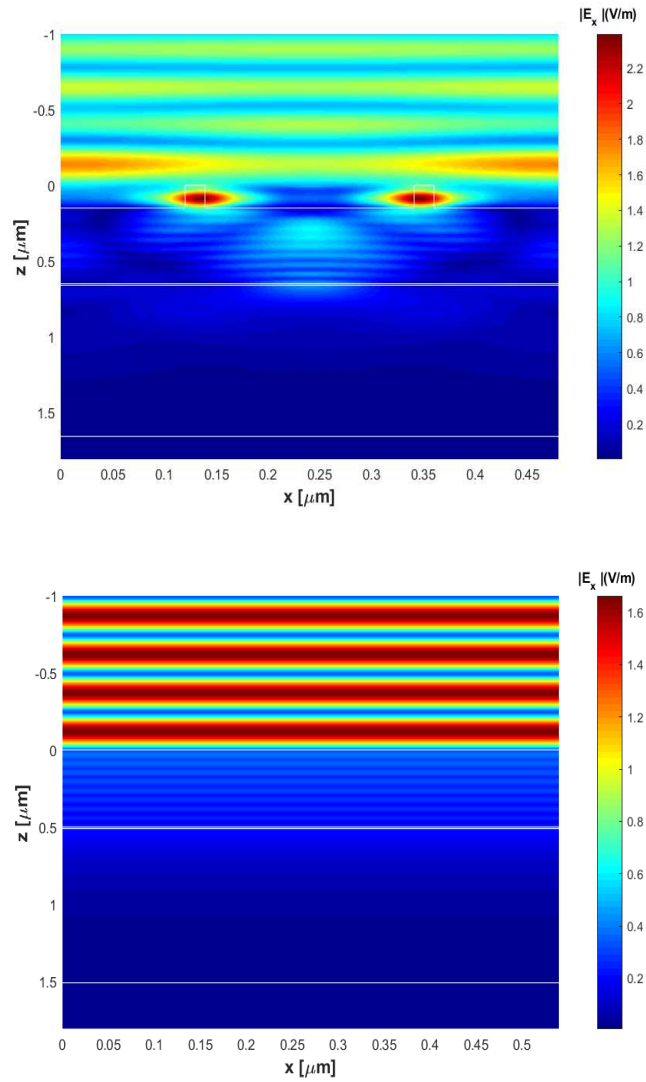


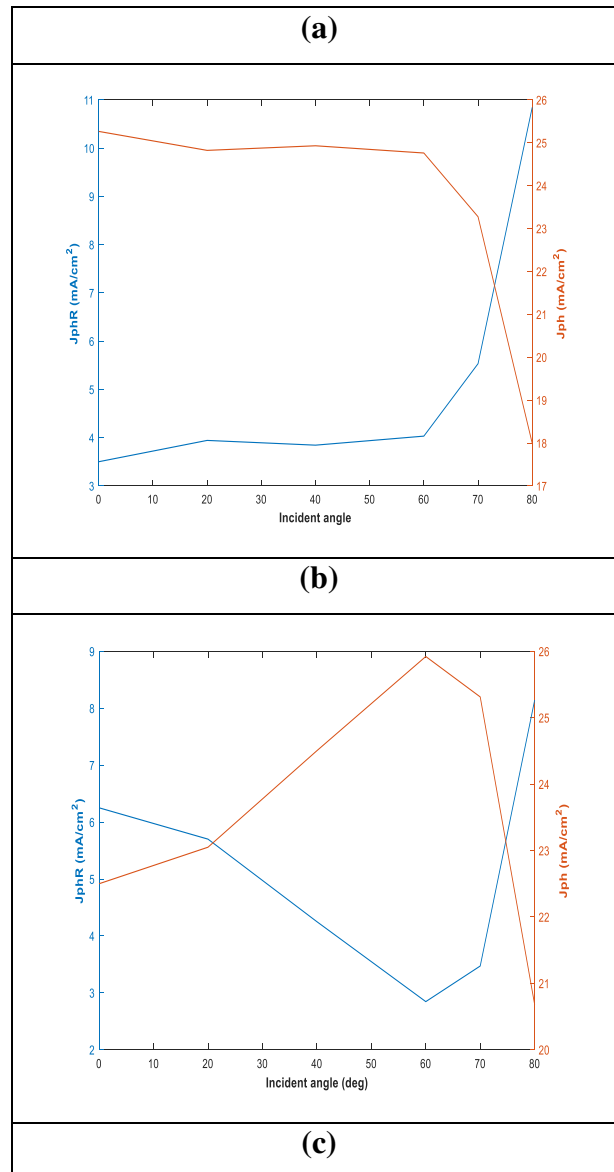
Figure 5: Component E_x of the electric field at a light wavelength of $0.5 \mu\text{m}$ for SC coated (a) and no-coated (b) by NTs array. The height, the diameter of NTs, the period of the array and the thickness of the CZTS layer are 150 nm , 240 nm , 480 nm and $1 \mu\text{m}$. The white lines are guides for the eyes to show the underlying nanowire structure described in Figure 1.

3- Variation of ideal current with the incident angle of the light

Taking the change in the sun's incidence angle into account, the relationship between J_{ph} and J_{phR} with the incident angle of light for different diameters of the NTs is illustrated in figure 6. The angle 0 corresponds to the normal incidence. We remark that for large diameter and small ratio P/D ($D=438 \text{ nm}$, $P/D=1$, figure 6-a) J_{ph} and J_{phR} are almost constant for incident angle smaller than 60° . Then, J_{phR} (J_{ph}) increases (decreases) rapidly. For smaller diameter or/and larger ratio P/D , with increasing the incident angle, J_{phR} (J_{ph}) decreases (increases) to reach a

minimum (maximum) then it increases. The incident angle corresponding to the minimum of J_{phR} shifts to a high value with increasing the ratio p/D .

It's worthy to note that figure 6a, which corresponds to the optimal geometrical parameters, shows that the NTs array still has good anti-reflection characteristics when the incident angle doesn't exceed 60° .



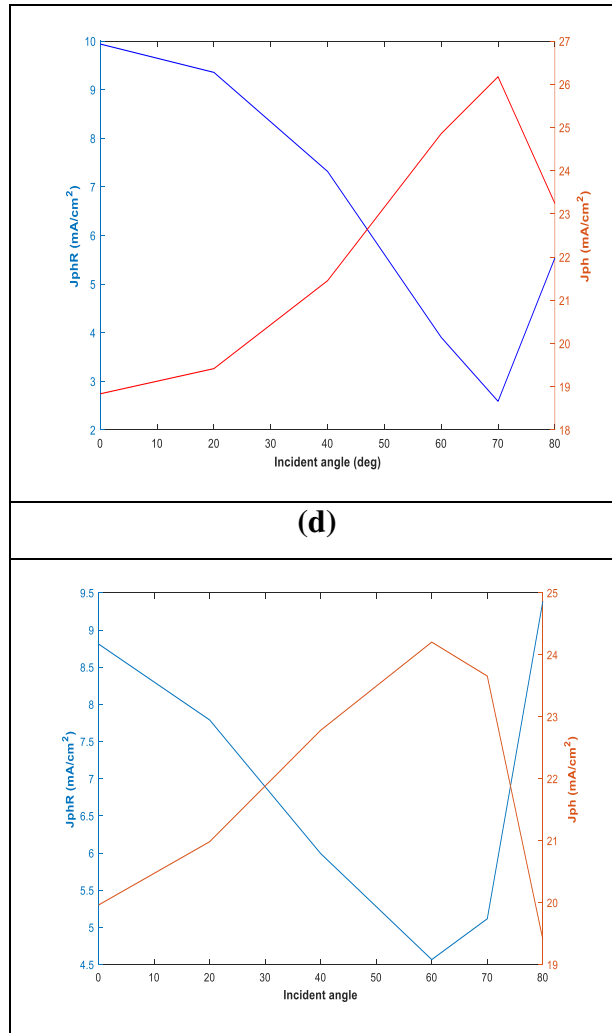


Figure 6: Variation of the ideal short circuit current density (J_{ph}) and of the lost ideal short circuit current density (J_{phR}) with the incident angle of light. The height of the NTs is 150 nm. The thickness of the CZTS layer is 1.5 μm . **(a)** The diameter of the NTs and the ratio P/D are 440 and 1 respectively. **(b)** The diameter of the NTs and the ratio P/D are 240 nm and 1 respectively. **(c)** The diameter of the NTs and the ratio P/D are 440 nm and 3 respectively. **(d)** The diameter of the NTs and the ratio P/D are 240 nm and 3 respectively

4- Conclusion

In this paper, we optically simulated a planar solar cell including Kesterite as a p-type absorber and Zinc Tin Oxide as an n-type buffer and coated by an antireflective coating composed of a ZnO square periodic nanotube array to optimize the structural morphology. An optimum value

of 42 mA/cm² for the ideal short circuit current density and a minimum value of 3.5 mA/cm² for the loss of ideal short circuit current density were found for diameter NTs of 438 nm, NTs height of 150 nm, array period of 438 nm and absorber thickness of 1.5 μm. Furthermore, the ideal short circuit current density is independent of the incident angle below 60°. We conclude that the coating with a ZnO NWs enhances considerably the performance of the studied solar cell.

References

- [1] Weintraub B, Chang S, Singamaneni S, HanWH, Choi YJ, Bae J, Kirkham M, Tsukruk VV, Deng Y., Density-controlled solution-based growth of ZnO nanorod arrays via layer-by-layer polymer thin films for enhanced field emission. *Nanotechnology* **19**, 435302 (2008). (doi:10.1088/0957-4484/19/43/435302)
- [2] Sun T, Qiu J, Liang C., Controllable fabrication and photocatalytic activity of ZnO nanobelt arrays. *J. Phys. Chem. C* **112**, 715 (2008). (doi:10.1021/jp710071f)
- [3] Wang JX, Sul XW, Yang Y, Huang H, Lee YC, Tan OK, Vayssieres L. 2006 Hydrothermally grown oriented ZnO nanorod arrays for gas sensing applications. *Nanotechnology* **17**, 4995. (doi:10.1088/0957-4484/17/19/037)
- [4] Wang HT, Kang BS, Ren F, Tien LC, Sadik PW, Norton DP, Pearton S, Lin J., Hydrogen-selective sensing at room temperature with ZnO nanorod. *Appl. Phys. Lett.* **86**, 243503 (2005). (doi:10.1063/1.1949707)
- [5] Kilinc N, Cakmak O, Kosemen A, Ermek E, Ozturk S, Yerli Y, Ozturk ZZ, Urey H., Fabrication of 1D ZnO nanostructures on MEMS cantilever for VOC sensor application. *Sens. Actuators B-Chem.* **202**, 357 (2014). (doi:10.1016/j.snb.2014.05.078)
- [6] Schlur L, Carton A, Lévêque P, Guillon D, Pourroy G., Optimization of a new ZnO nanorods hydrothermal synthesis method for solid state dye sensitized solar cells applications. *J. Phys. Chem. C* **117**, 2993 (2013). (doi:10.1021/jp305787r)
- [7] Son DY, Im JH, Kim HS, Park NG., 11% Efficient perovskite solar cell based on ZnO nanorods: an effective charge collection system. *J. Phys. Chem. C* **118**, 16567 (2014). (doi:10.1021/jp412407j)
- [8] Melliti A., Optical simulation of solar cell based on ZnO/ZTO core-shell nanowire array embedded in CZTS layer, *Optical and Quantum Electronics* **53**, 91 (2021), (doi: 10.1007/s11082-021-02738-w)

- [9] Melliti A., Optical simulation of solar cell based on ZnO/ZTO core-shell nanowire array embedded in CZTS layer, *Optical and Quantum Electronics* (submitted).
- [10] Varadharajaperumal S., Alagarasan D., Ganesan R., Satyanarayan M.N., Hegde G., Controlled growth of 1D-ZnO nanotubes using one-step hot plate technique for CZTS heterojunction solar cells, *Materials Science in Semiconductor Processing* 106, 104763 (2020), (doi: 10.1016/j.mssp.2019.104763)
- [11] Chung Ch.-Ch., Tran B.T., Lin K.-L., Ho T.-T., Yu H.-W., Quang N.-H., Chang E.Y., Efficiency improvement of InGaP/GaAs/Ge solar cells by hydrothermal-deposited ZnO nanotube structure, *Nanoscale Res. Lett.* 9, 338 (2014) (10.1186/1556-276X-9-338).
- [12] Cui X., Sun K., Huang J., Lee C.-Y., Yan C., Sun H., Zhang Y., Liu F., Hossain Md. A., Zakaria Y., Wong L. H., Green M., Hoex B., and Hao X., Enhanced Heterojunction Interface Quality To Achieve 9.3% Efficient Cd-Free $\text{Cu}_2\text{ZnSnS}_4$ Solar Cells Using Atomic Layer Deposition ZnSnO Buffer Layer, *Chem. Mater.* 30, 7860 (2018). (doi: 10.1021/acs.chemmater.8b03398)
- [13] Green M. A., Hishikawa Y., Dunlop E. D., Levi D. H., Hohl-Ebinger J., Ho-Baillie A. W. Y., Solar cell efficiency tables (version 52). *Prog. Photovoltaics Res. Appl.*, 26, 427 (2018) doi: 10.1002/pip.3040).
- [14] Li L., New formulation of the Fourier modal method for crossed surface-relief gratings, *J. Opt. Soc. Am. A* 14, 2758 (1997) (doi: 10.1364/JOSAA.14.002758).
- [15] Mullings M. N., Hägglund C., Tanskanen J. T., Yee Y., Geyer S., Bent S. F., Thin film characterization of zinc tin oxide deposited by thermal atomic layer deposition, *Thin Solid Films* 556, 186 (2014) (doi: 10.1016/j.tsf.2014.01.068).
- [16] Gorji Nima E., Quantitative Analysis of the Optical Losses in CZTS Thin-Film Semiconductors, *IEEE TRANSACTIONS ON NANOTECHNOLOGY* 13, 743 (2014) (doi: 10.1109/TNANO.2014.2318057).
- [17] Michallon J., Zanucoli M., Kaminski-Cachopo A., Consonni V., Morand A., Bucci D., Emieux F., Szabolcs H., Perraud S., Semenikhin I., Comparison of optical properties of Si and ZnO/CdTe core/shell nanowire arrays, *Materials Science and Engineering B* 178, 665 (2013) (doi: 10.1016/j.mseb.2012.10.037).

- [18] Thomas R., Mathavan T., Jothirajan M.A., Somaily H.H., Zahran H.Y., Yahia I.S., An effect of lanthanum doping on physical characteristics of FTO thin films coated by nebulizer spray pyrolysis technique, *Optical Materials* 99, 109518 (2020) (doi: 10.1016/j.optmat.2019.109518).
- [19] ASTM, Reference Solar Spectral Irradiance: Air Mass 1.5 Spectra, <http://rredc.nrel.gov/solar/spectra/am1.5> (2020).

Figures

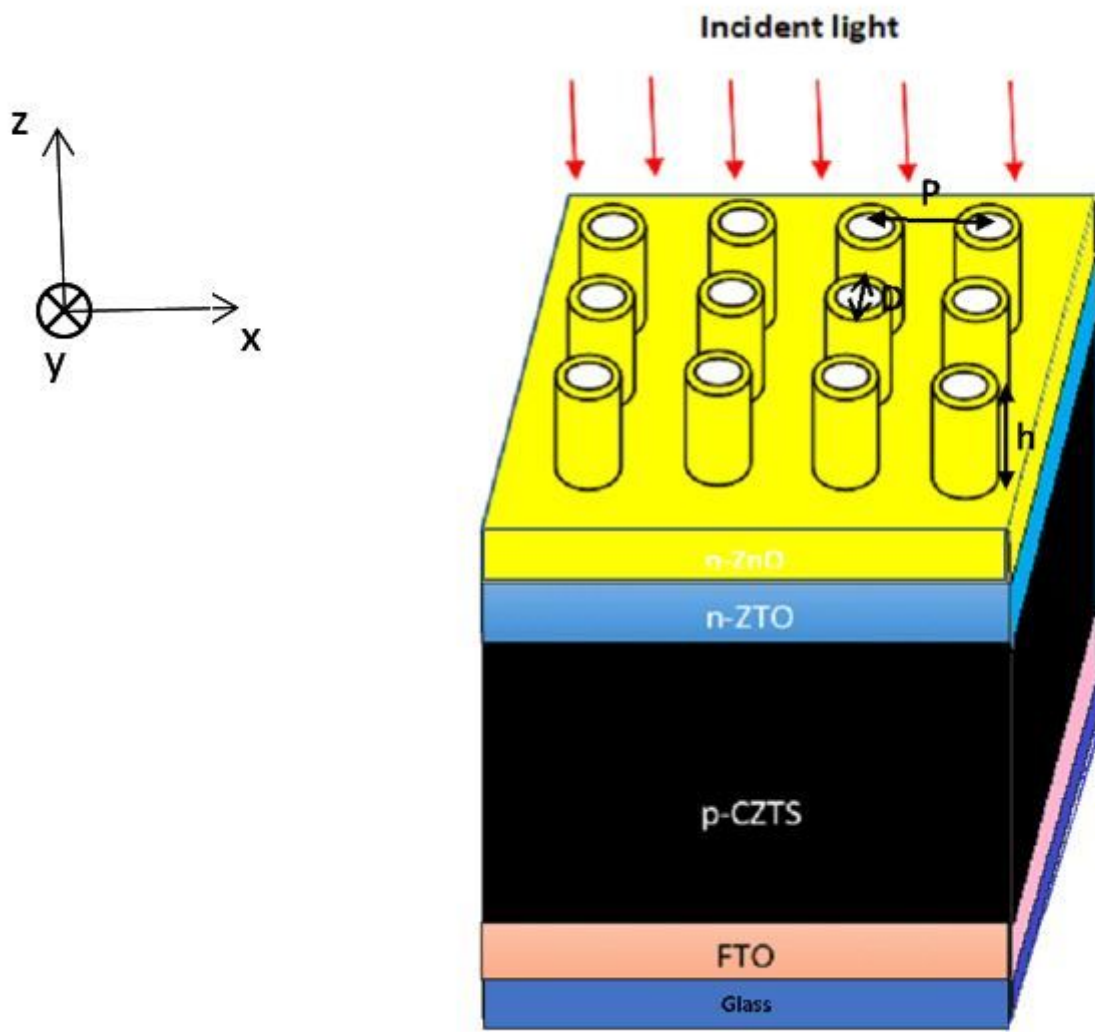


Figure 1

Structure of the planar SC including CZTS as p-type absorber and ZTO as n-type buffer with a ZnO NTs array as an anti-reflector.

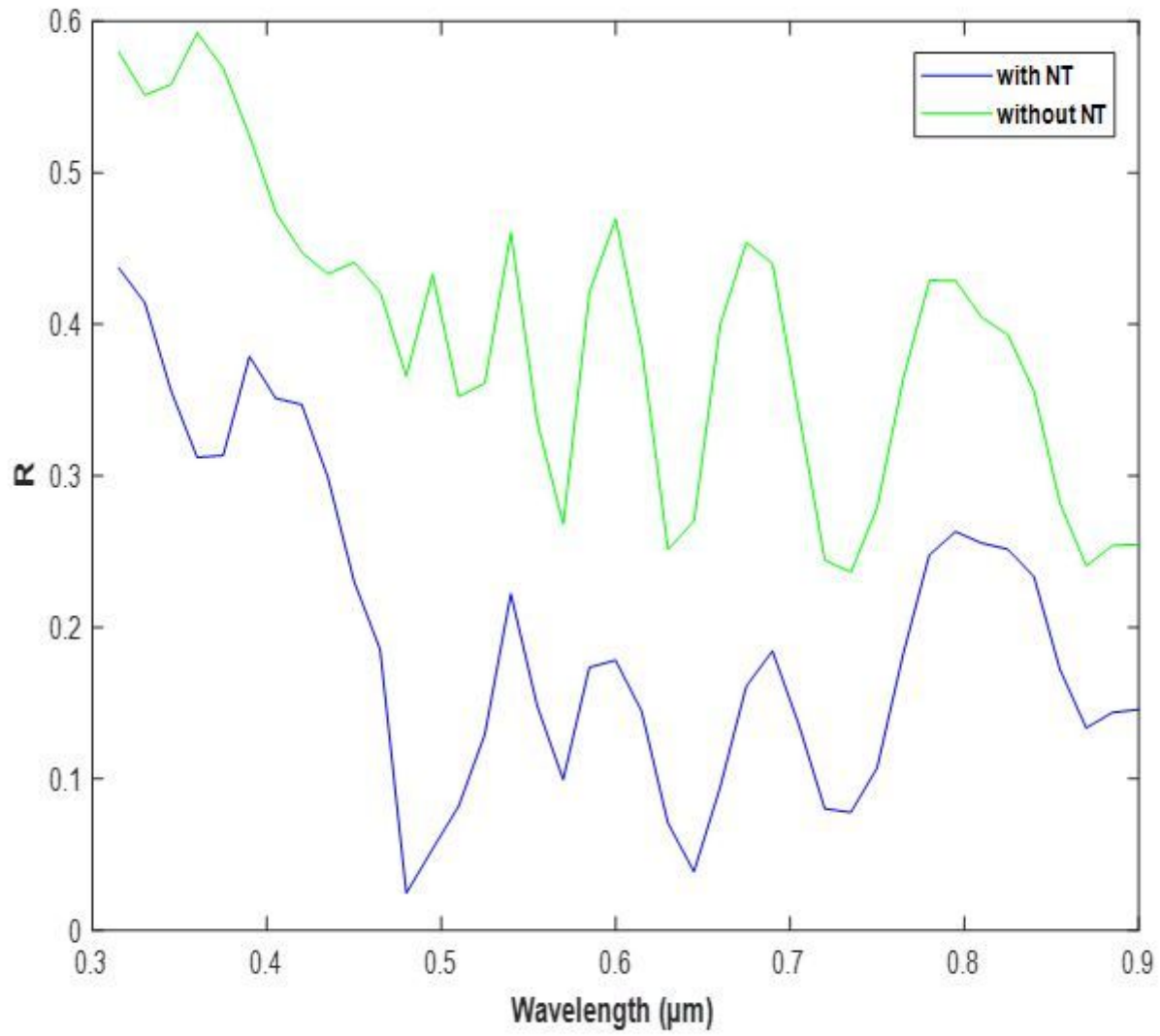


Figure 2

Reflectance spectra of SCs with and without NTs array. The height, the diameter of NTs, the period of the array and the thickness of the CZTS layer are 150 nm, 240 nm, 480 nm and 1 μm.

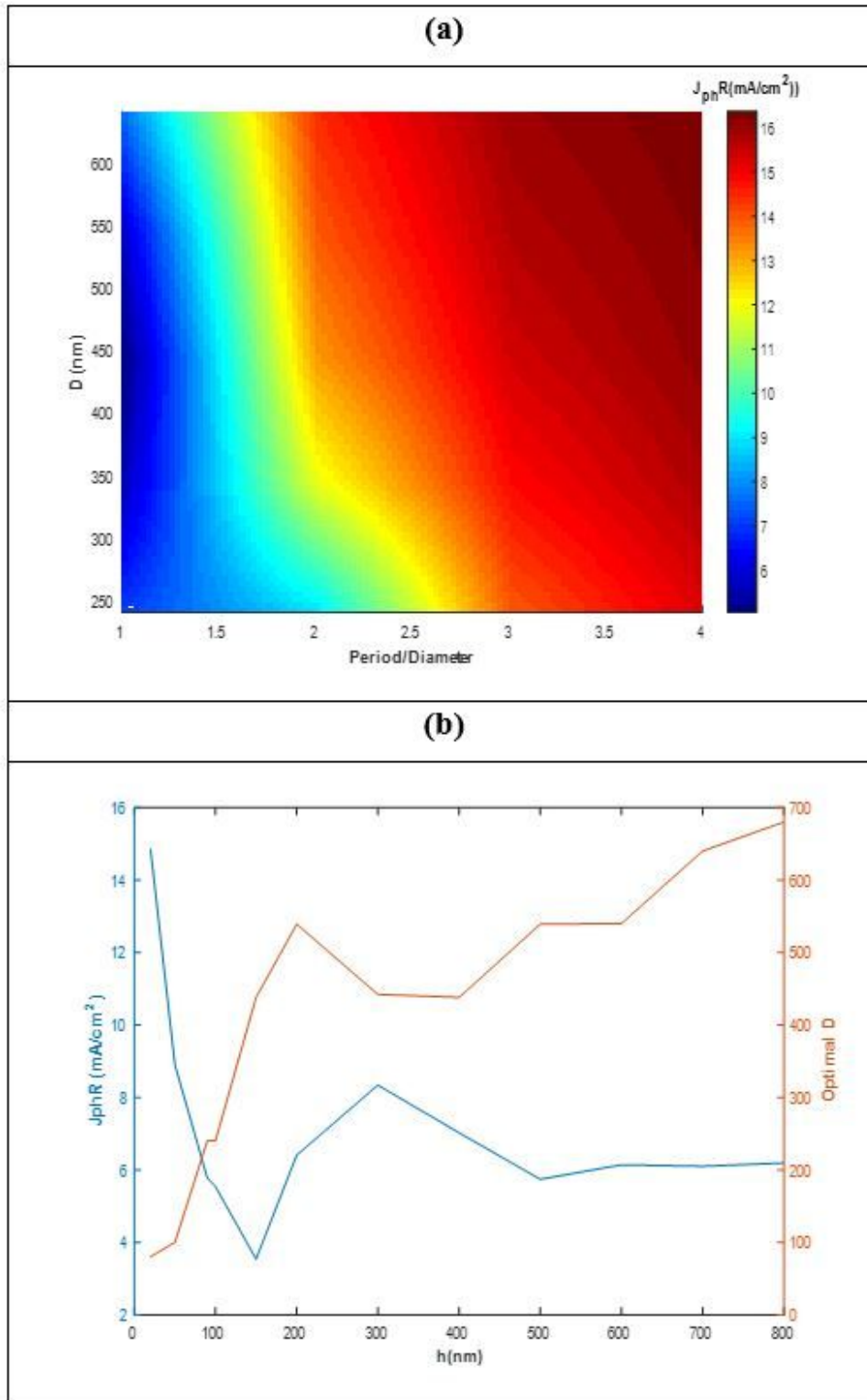


Figure 3

(a) Lost ideal short circuit current density (J_{phR}) computed for $h = 150$ nm as a function of the diameter of NTs (D) and the ratio between the array period P and the diameter D of the NTs. The 20 data points map has been linear interpolated on a 500 times larger grid. The thickness of the CZTS layer is $1 \mu\text{m}$. (b) Evolution of the optimal value of the NTs diameter and the corresponding value of J_{phR} as a function of NTs height (h).

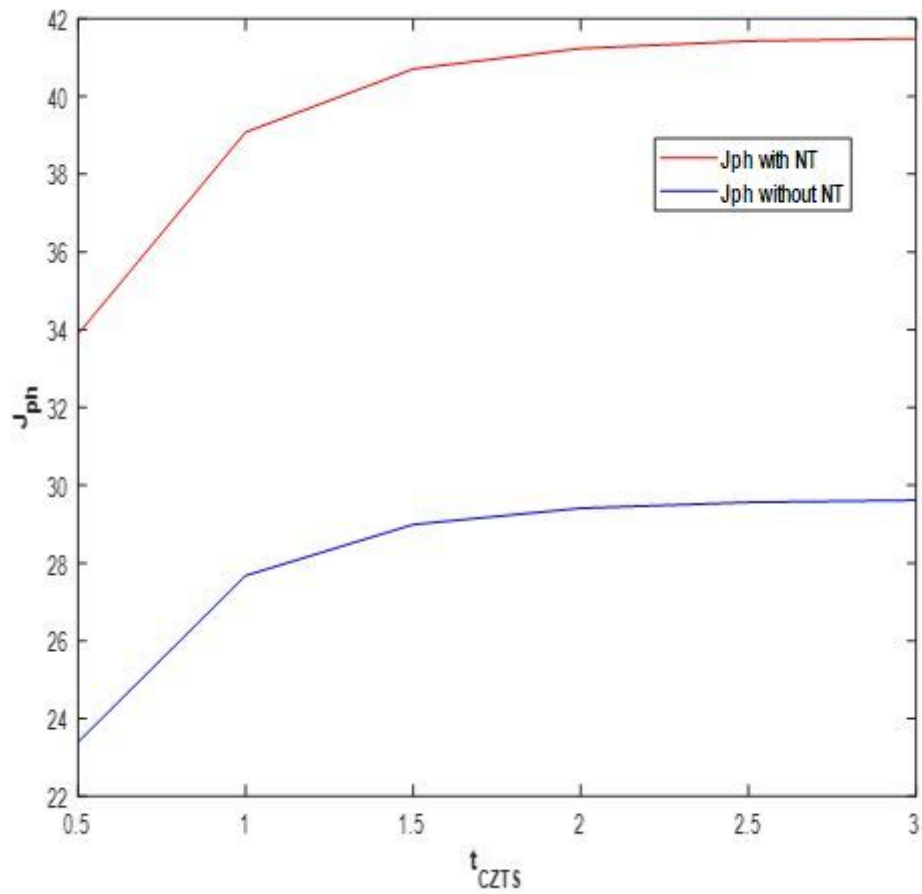


Figure 4

Variation of ideal short circuit current density (J_{ph}) obtained for the optimal values of D and P/D as a function of the thickness of the CZTS layer (t_{CZTS}).

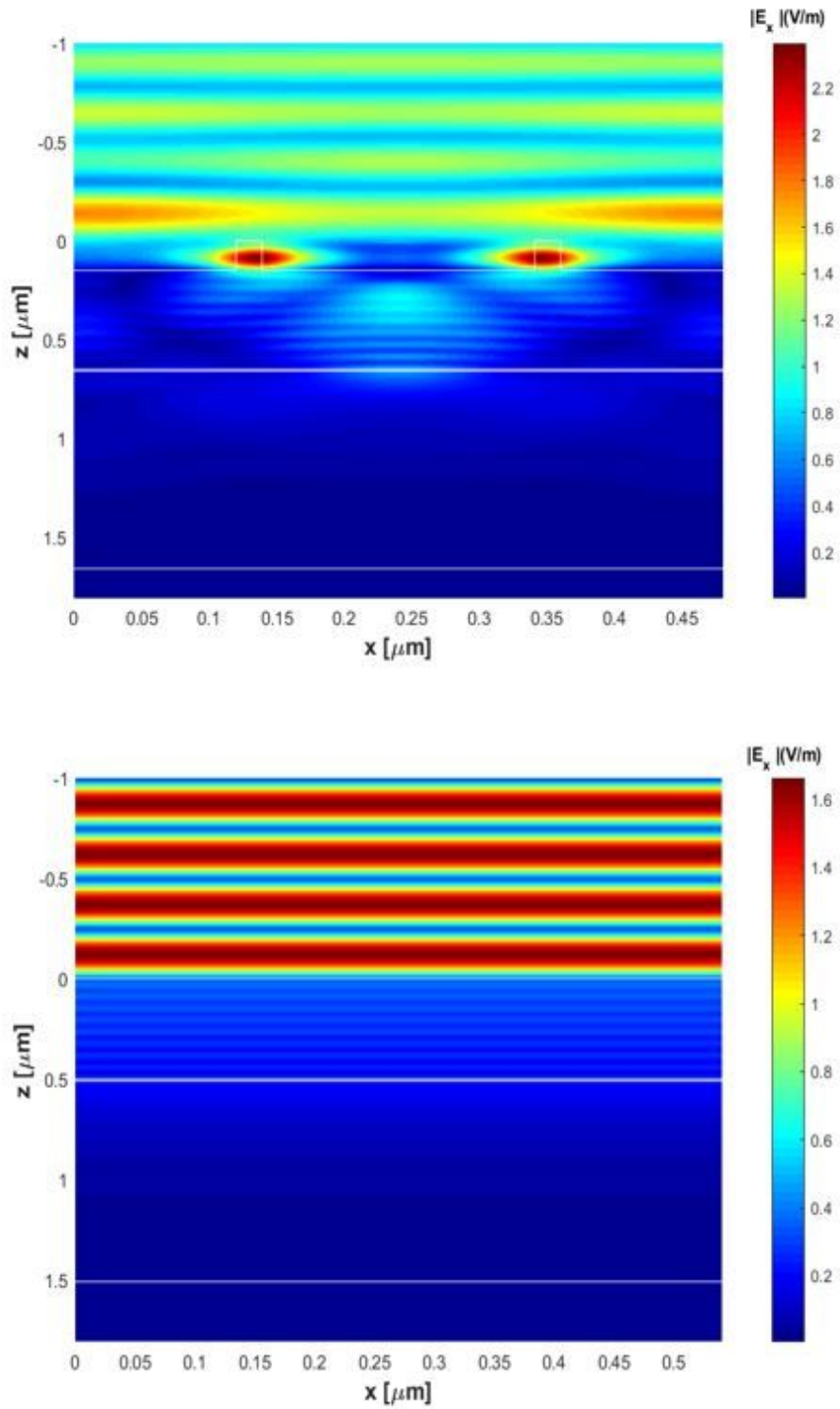


Figure 5

Component E_x of the electric field at a light wavelength of $0.5 \mu\text{m}$ for SC coated (a) and no-coated (b) by NTs array. The height, the diameter of NTs, the period of the array and the thickness of the CZTS layer are 150 nm , 240 nm , 480 nm and $1 \mu\text{m}$. The white lines are guides for the eyes to show the underlying nanowire structure described in Figure 1.

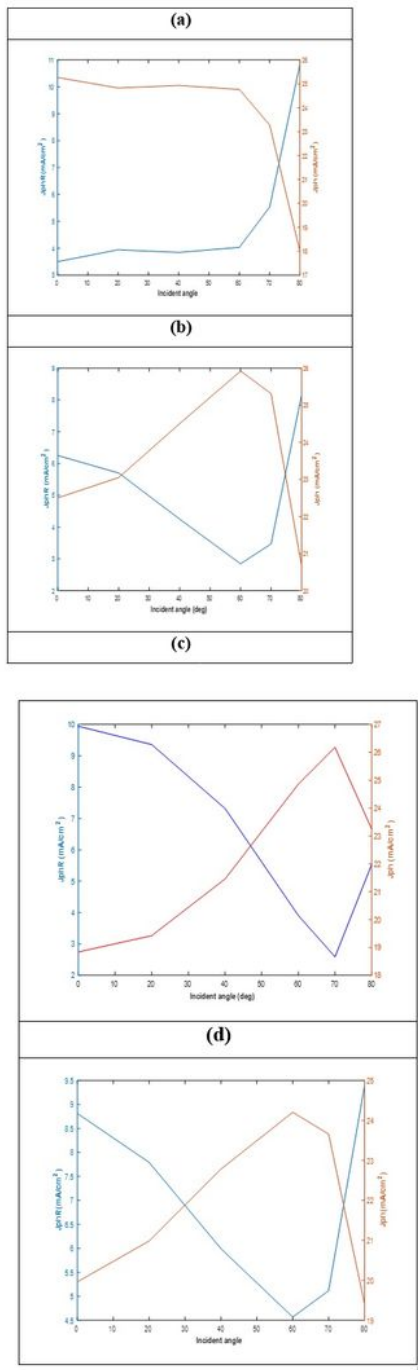


Figure 6

Variation of the ideal short circuit current density (J_{ph}) and of the lost ideal short circuit current density (J_{phR}) with the incident angle of light. The height of the NTs is 150 nm. The thickness of the CZTS layer is 1.5 μm . (a) The diameter of the NTs and the ratio P/D are 440 and 1 respectively. (b) The diameter of the NTs and the ratio P/D are 240 nm and 1 respectively. (c) The diameter of the NTs and the ratio P/D

are 440 nm and 3 respectively. (d) The diameter of the NTs and the ratio P/D are 240 nm and 3 respectively